

Thermal Evolution of Calcium Aluminate Gel Obtained from Aluminium Sec-Butoxide Chelated with Ethyl Acetoacetate

S. Kurajica*, V. Mandić and J. Šipusić

University of Zagreb, Faculty of Chemical Engineering and Technology, 19 Marulićev trg, Zagreb, Croatia
received May 25, 2010; received in revised form July 6, 2010; accepted September 23, 2010

Abstract

Calcium aluminate (CaAl_2O_4) powder was prepared with a sol-gel technique using calcium nitrate tetrahydrate and aluminium sec-butoxide as precursors and ethyl acetoacetate as chelating agent. The dried gel and thermally treated samples were characterized by means of simultaneous Differential Thermal and Thermo-Gravimetric Analysis (DTA/TGA), Fourier Transform Infrared spectroscopy (FTIR), and X-Ray Diffraction (XRD). From the results obtained, the thermal evolution of the prepared gel, the crystallization behaviour and crystallization kinetics are discussed. It has been established that the decomposition of the chelate and the evaporation of ethyl acetoacetate followed by an auto-combustion process occur in a lower temperature range. The crystallization process starts at temperatures higher than 900 °C. Calcium aluminate, CaAl_2O_4 , appears as the major crystalline phase, and calcium dialuminate, CaAl_4O_7 , and dodecacalcium heptaaluminate, $\text{Ca}_{12}\text{Al}_{14}\text{O}_{33}$, as minor phases. The crystallization processes of the phases proceed simultaneously and independently. Thermal treatment at higher temperature increases the amount of calcium aluminate and decreases the amount of minor components.

Keywords: Calcium aluminate, sol-gel, thermal evolution, crystallization, non-isothermal kinetics.

I. Introduction

Calcium aluminate, CaAl_2O_4 , (CA in cement notation) is the main crystalline phase of aluminate cement and an important refractory material. Crystalline calcium aluminates are also used in high-strength and high-toughness ceramic-polymer composite materials¹. CA also plays an important role in the processing and performance of chemically bonded ceramics². Recently, new applications for calcium aluminates have emerged in optical ceramics and information storage devices³. In addition, it has been demonstrated that CA has bioactive properties and CA-based materials have been investigated as bioactive dental materials⁴.

For advanced applications high-purity CA is required. The preparation of pure CA phase is also of importance for fundamental research in cement chemistry. The aluminate cement clinker is a quite complex system of multiple binary and ternary phases, and the interpretation of investigation results in such systems is difficult, sometimes even impossible. Therefore, the use of pure CA enables a deeper insight into the hydration process kinetics and into the influence of minor elements and additives on the reactivity of cement⁵.

The traditional technique of preparing pure calcium aluminate compounds is based on solid-state reactions (sintering) of calcium and aluminium oxides (or oxide precursors such as carbonates or oxalates). Precursors are physically mixed, held at high temperatures (required for the

solid-state diffusion process) for an extended time, ground and re-sintered.

Almost all previous investigations of this process agree that the kinetic mechanism is based on a diffusion-controlled rate-determining step⁶. The reported values of the activation energies for the formation of monocalcium aluminate are in the range of 152 to 502 kJ mol⁻¹. Literature values for the activation energy vary widely owing to differences in the precursor compounds and particle size distribution. Slightly lower values have been obtained for the crystallization from the amorphous precursor (118 kJ mol⁻¹)⁷ and higher for the crystallization of CA glass (569 kJ mol⁻¹)⁸.

The solid-state process takes from a few hours up to several days with intermediate grinding⁵ and still does not allow fine control of the phase composition and the microstructure owing to limitations of physical mixing to the micrometer scale, yielding multiple, unwanted phases¹. Therefore, the advanced CA applications such as fibres, thin films and coatings require a sophisticated preparation process.

Various chemical approaches have been developed for the synthesis of pure, single-phase calcium aluminate powders: e.g. Pechini process⁷, evaporation¹, spray-drying², self-propagating high-temperature synthesis (combustion synthesis)⁹ and sol-gel⁵.

In order to provide a more efficient method for the synthesis of pure phases, the sol-gel process was introduced to synthesize amorphous calcium aluminate powders^{3,10-12}. The sol-gel method is a wet-chemical process that is advantageous compared to solid-state reaction methods.

* Corresponding author: e-mail: stankok@fkit.hr

Such advantages have been related to good mixing of starting reagents yielding more homogeneous products with greater reactivity. Consequently, crystallization is achieved by subsequent heating of the amorphous gel at lower processing temperature.

Alkoxides are often used as precursors in sol-gel synthesis. Aluminium alkoxides, such as aluminium sec-butoxide, are known for their high affinity for water. Uncontrolled hydrolysis of these precursors results in an aluminium hydroxide precipitate¹³. In order to achieve control over sol-to-gel transformation, the alkoxide hydrolysis rate has to be controlled. Chemical modification of metal alkoxide with chelating agents such as β -diketones is known to be very effective for the control of reactivity and condensation process of reactive metal alkoxides¹³⁻¹⁵. A replacement of the reactive alkoxy group with a less hydrolysable entity reduces the rate of hydrolysis^{13,16}.

Alkoxides are often used as precursors in sol-gel synthesis. Aluminium alkoxides, such as aluminium sec-butoxide, are known for their high affinity for water. Uncontrolled hydrolysis of these precursors results in an aluminium hydroxide precipitate¹³. In order to achieve control over sol-to-gel transformation, the alkoxide hydrolysis rate has to be controlled. Chemical modification of metal alkoxide with chelating agents such as β -diketones is known to be very effective for the control of reactivity and condensation process of reactive metal alkoxides¹³⁻¹⁵. A replacement of the reactive alkoxy group with a less hydrolysable entity reduces the rate of hydrolysis^{13,16}.

Sol-gel synthesis of CA from calcium nitrate tetrahydrate and aluminium sec-butoxide, chelated with ethyl acetoacetate in various ratios, and spectroscopic study of obtained gels has been the subject of our previous investigation¹⁷. In this work thermal evolution of calcium aluminate gel obtained from aluminium sec-butoxide chelated with ethyl acetoacetate was reported.

II. Experimental

Precursor materials used to prepare the gel were aluminium sec-butoxide, Asb ($\text{Al}(\text{O}^i\text{Bu})_3$, 97 %, Aldrich, Great Britain), ethyl acetoacetate, Eaa ($\text{C}_6\text{H}_{10}\text{O}_3$, 99 %, Fluka, Germany) and $\text{Ca}(\text{NO}_3)_2 \cdot 4\text{H}_2\text{O}$ (p.a. assay, Kemika, Croatia). Isopropyl alcohol ($\text{C}_3\text{H}_7\text{OH}$, 99 %, Kemika, Croatia) was used as a solvent as it was experimentally proven to be a good mutual solvent for the Asb-Eaa system¹³. All chemicals were used as received.

First, the Eaa was added to the solvent and then the appropriate amount of Asb was dissolved in solvent/Eaa solution. Asb was added to the solution using a syringe to minimize exposure to air humidity. Upon addition of Asb to the Eaa/solvent solution, the exothermic process occurs. The appropriate amount of $\text{Ca}(\text{NO}_3)_2 \cdot 4\text{H}_2\text{O}$ was dissolved in the solvent separately. Both solutions were stirred for 1 h before the $\text{Ca}(\text{NO}_3)_2 \cdot 4\text{H}_2\text{O}$ solution was added drop-wise to the Eaa/Asb solution. The molar ratio of Asb : Eaa : $\text{Ca}(\text{NO}_3)_2 \cdot 4\text{H}_2\text{O}$: solvent was 2 : 3 : 1 : 10. No water was added except for that contained in $\text{Ca}(\text{NO}_3)_2 \cdot 4\text{H}_2\text{O}$. No precipitation was observed after the solution was stirred for 24 h at room temperature.

The clear sol was poured into a large Petri dish in order to maximize the exposure to air moisture, and kept at

room temperature. After two days, gelation occurred, and a completely transparent gel was obtained. Drying of the sample for five more days at room temperature enabled the evaporation of solvent and the release of alkoxy groups, resulting in a dry product. The obtained sample was subsequently ground to a fine powder and stored. The measurements were conducted approximately 1 month after the synthesis.

The thermal behaviour of powder precursors was characterized with Differential Thermal Analysis (DTA) and Thermo-Gravimetric Analysis (TGA) using the Netzsch STA 409 simultaneous DTA/TGA analyzer. For the thermal analysis, ~50 mg of material was placed in Pt crucibles and heated at the rate of $10^\circ\text{C min}^{-1}$ to 1000°C in a synthetic air flow of $30\text{ cm}^3\text{ min}^{-1}$, with α -alumina as a reference.

IR spectra of the samples were acquired using the Bruker Vertex 70 Fourier transform infrared spectrometer in ATR (attenuated total reflectance) mode. The samples were pressed on a diamond and the absorbance data were collected between 400 and 4000 cm^{-1} with spectral resolution of 1 cm^{-1} and 64 scans.

The crystal phases were identified by means of powder X-ray diffraction (XRD) using a Philips diffractometer PW 1830 with $\text{CuK}\alpha$ radiation. Data were collected between 5 and $70^\circ 2\theta$ in a step scan mode with steps of 0.02° and counting time of 5 s.

In order to assign the peaks on DTA scan, DTA analysis was performed at the rate of $10^\circ\text{C min}^{-1}$. The analysis was stopped at successively higher temperatures; the sample was quenched and analyzed by means of XRD and FTIR. The same procedure was applied in order to determine the crystallization path. Si was added as an internal standard.

For the purpose of kinetic evaluation, DTA analysis was performed at five different heating rates (2, 4, 8, 16 and $32^\circ\text{C min}^{-1}$).

The applicability of the JMA model for description of crystallization kinetics has been tested using Malek's method¹⁸. Further kinetic analysis has been based upon the Kissinger-Akahira-Sunose (KAS) equation^{19,20}.

III. Results

DTA, TGA, DTG traces of calcium aluminate gel are shown in Fig. 1. DTA trace shows one endothermic peak in the range between room temperature and 230°C followed by a sharp exothermic peak between 230°C and 310°C . At higher temperatures, the DTA trace shows an additional faint exotherm between 900°C and 970°C . From TGA and DTG traces it can be seen that there are three principal regions where weight loss occurs. The initial weight loss of 45.1 % in the temperature range between room temperature and 229°C , rapid weight loss of 27.6 % between 229 and 232°C and additional weight loss of 2.8 % between 232°C and 1000°C . The total weight loss according to TG curve is 75.5 %

In order to assign DTA and DTG peaks, the DTA analysis of the sample was stopped at 200°C and 300°C , the samples were quenched and analyzed by XRD and FTIR. Infra-red spectra of the dried sample and the samples quenched from 200°C and 300°C are presented in Fig. 2.

Eaa belongs to a group of β -ketoesters that are capable of undergoing keto-enol tautomerism. In pure Eaa the ketonic form predominates²¹. In the presence of Asb the reactive enol form of Eaa substitutes the alkoxy groups of Asb. Formation of the chelate strongly shifts the keto-enolic equilibrium towards the enolic form stabilized by the chelation with Asb²¹. The spectrum of the dried sample exhibits characteristic absorption bands of Eaa in the chelate at $\sim 1610\text{ cm}^{-1}$ due to a C-O in enolic form bonded to Al and band at $\sim 1525\text{ cm}^{-1}$ due to a C-C vibration of six membered ring of the complex^{14,15}. The spectrum shows no bands due to the ketonic form of Eaa occurring at $1753\text{--}1718\text{ cm}^{-1}$ owing to the C=O stretching vibration of two carbonyl groups^{14,15}. The spectrum also exhibits bands at: 1475 cm^{-1} (asymmetrical bending vibration of the C-H bonds), 1415 cm^{-1} (C-H rocking vibration), and 1369 cm^{-1} (symmetrical bending vibration of the C-H bonds). A series of bands in the region

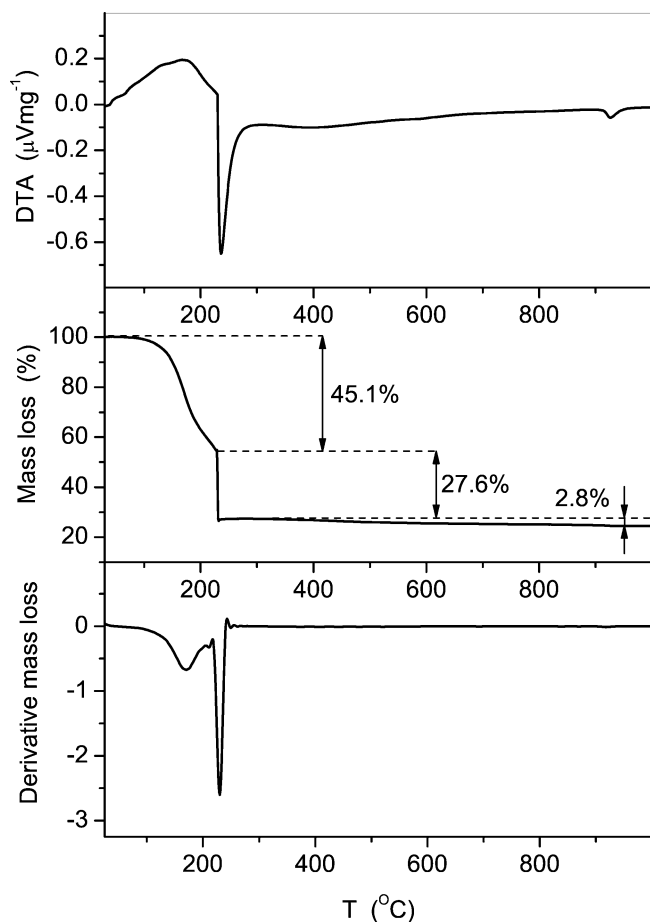


Fig. 1: DTA, TGA, DTG traces of dried gel.

$1350\text{--}1150\text{ cm}^{-1}$ is characteristic for esters, as a result of methylene twisting and wagging vibrations²². The major absorption bands due to NO_3^- groups²² are located at 1305 , 1445 and 1630 cm^{-1} , mostly overlapped with Eaa bands. The FTIR spectra presented in Fig. 2 show that Eaa reacts with Asb, forming a chelate, and that Eaa groups in the chelate are resistant to hydrolysis. The spectrum of the sample thermally treated at 200°C also exhibits characteristic absorption bands of Eaa in chelate but with reduced intensity. It seems that chelate decomposition and evaporation of Eaa starts before 200°C . The adsorbed water

and some possible remains of the solvent also evaporate in this temperature interval. The sample thermally treated at 300°C (after the exothermic peak and rapid mass loss) shows only weak bands owing to NO_3^- groups.

Fig. 3 shows the XRD patterns of the dried sample and samples quenched from 200°C and 300°C . The XRD pattern of the dried sample shows the diffraction peaks of two phases. One phase is identified as $\text{Ca}(\text{NO}_3)_2 \cdot 4\text{H}_2\text{O}$ (ICDD-PDF No.49-1105). The other phase is not listed in the ICDD-PDF database but, according to FTIR spectroscopy results, it could be assumed that it is related to Asb-Eaa chelate. XRD peaks assigned to an Asb-Eaa chelate showed reduced intensities in the pattern of the sample treated at 200°C and completely disappear in the pattern of the sample treated at 300°C . The nitrate peaks are unchanged in the pattern of the sample treated at 200°C and reduced in intensity in the pattern of the sample treated at 300°C . The FTIR spectra corroborate with XRD results showing reduced intensity of chelate bands for the sample treated at 200°C and broad bands due to NO_3^- for the sample treated at 300°C , which were overlapped with Eaa bands in other samples.

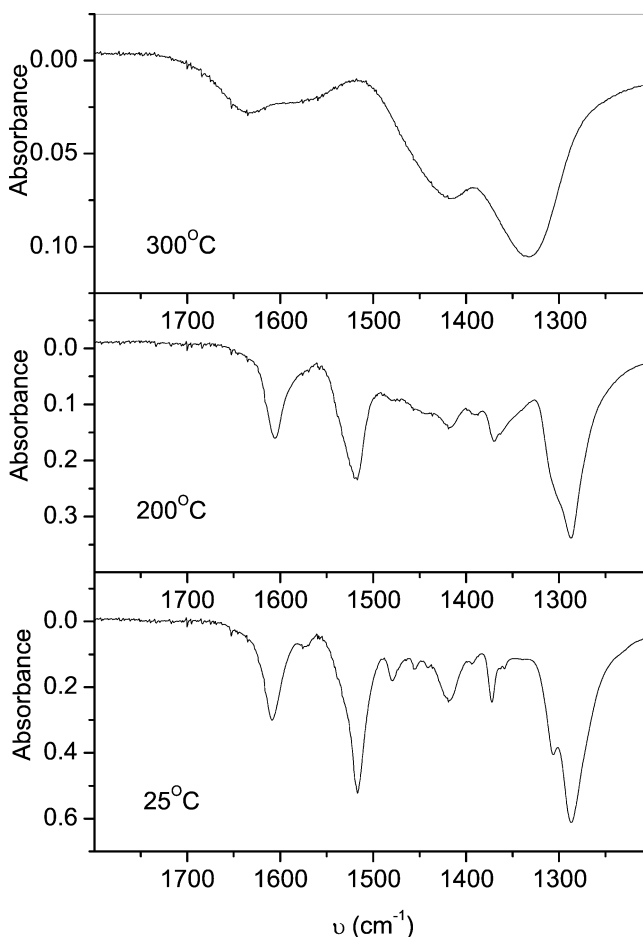


Fig. 2: IR spectra of dried gel, and samples thermally treated at 200°C and 300°C .

According to results of XRD and FTIR analysis, the decomposition of chelate and the evaporation of ethyl acetoacetate can be associated with the first endothermic peak in DTA scan and initial weight loss. This finding relates well with literature: according to Gonzales-Pena *et al.*²³, the decomposition of ethyl acetoacetate complexes is

shown to take place at around 210 °C. According to Jackson *et al.*²⁴, thermally induced decomposition of Eaa occurs at temperatures higher than 180 °C and C. Jing *et al.*²⁵ also attributed an endothermic peak with the maximum at 180 °C to the evaporation of solvent and Eaa. The evaporation of physically adsorbed water also occurs. There is no evidence of the existence of other organic residues (solvent or butanol) in the sample but evaporation of the traces of this species cannot be excluded. Sharp exothermic peak and abrupt mass loss in very narrow temperature range indicate the occurrence of auto-combustion process²⁶. A thermally induced anionic redox reaction occurs in which carboxyl groups act as reductant and NO_3^- ions act as oxidant²⁷. The decomposition of Eaa complexes followed by the decomposition of Eaa could promote an auto-combustion process. The additional weight lost at higher temperatures could be attributed to removal of unreacted nitrate²⁸ and to the pyrolysis of residual carbon formed during rapid combustion process²⁷. The presence of residual carbon is obvious from the greyish colour of the powder after quenching from 300 °C.

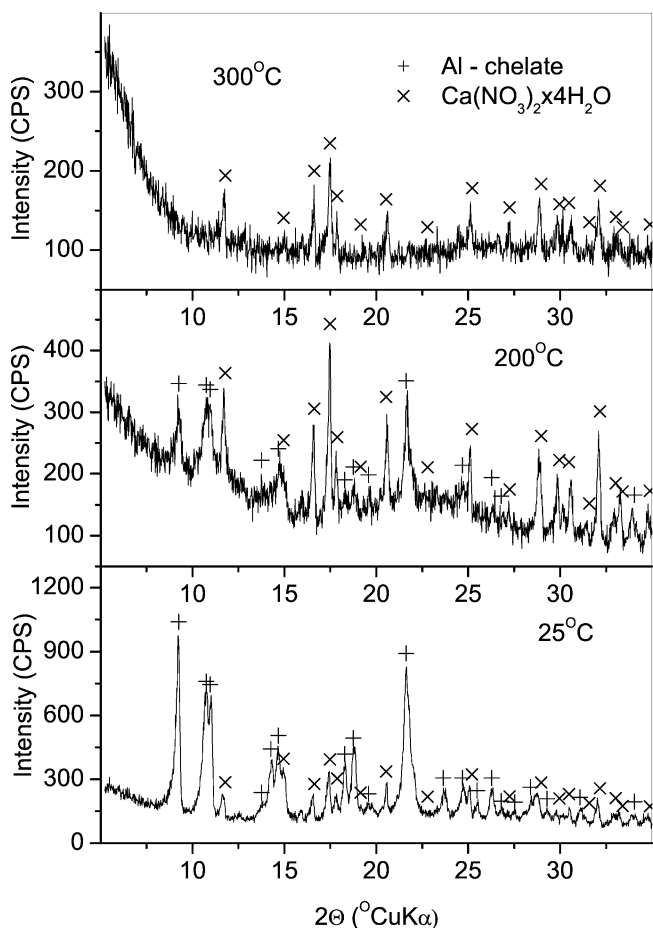


Fig. 3: Powder X-ray diffraction patterns of dried gel, and samples thermally treated at 200 and 300 °C.

The sample was thermally treated in a furnace in static air at a heating rate of 10 °Cmin⁻¹ and a firing temperature of 700 °C and 1000 °C for 2 h. Fig. 4 shows XRD patterns of fired samples. The sample thermally treated at 700 °C shows only a broad hill ranging approximately from 20 to 40 ° 2θ CuKα, indicating that the sample is completely amorphous. When the sample was annealed at 1000 °C,

crystallization occurs. The sample thermally treated at 1000 °C presented three crystal phases which were identified as calcium aluminate, CaAl_2O_4 (CA) (ICDD-PDF No. 23-1036), as the major crystalline phase, and calcium dialuminate, CaAl_4O_7 (CA_2) (ICDD-PDF No. 23-1037) and dodecacalcium heptaaluminate, $\text{Ca}_{12}\text{Al}_{14}\text{O}_{33}$ (C_{12}A_7) (ICDD-PDF No. 48-1882), as minor phases. The direct crystallization of calcium aluminate powders obtained by various chemical processing techniques into pure corresponding crystalline phases is rather difficult and rarely reported. A high number of compounds exists for this binary oxide system and the reasons for occurrence of minor phases proposed in literature are: local chemical variations in the composition of the precursors originating from sol segregation⁷, inhibition of long-range diffusion of cations at moderate temperatures² and more rapid kinetics of other phases³. Zawrah *et al.*²⁹ noted that the formation sequence of phases in mixtures of CaO and Al_2O_3 was always from calcia-rich phases to the proportioned phases. In a batch that is proportioned for CA single-phase calcium aluminate was produced only after prolonged reaction time at high temperatures. Sing *et al.*³⁰ explained this behaviour with the higher reactivity of CaO with respect to Al_2O_3 . In a study concerned with the sequence of phases formed during the formation of CA, Scian *et al.*³¹ reported that the reaction proceeded through the formation of multiple aluminates. C_{12}A_7 was formed first and subsequently reacted with CA_2 and alumina to form CA.

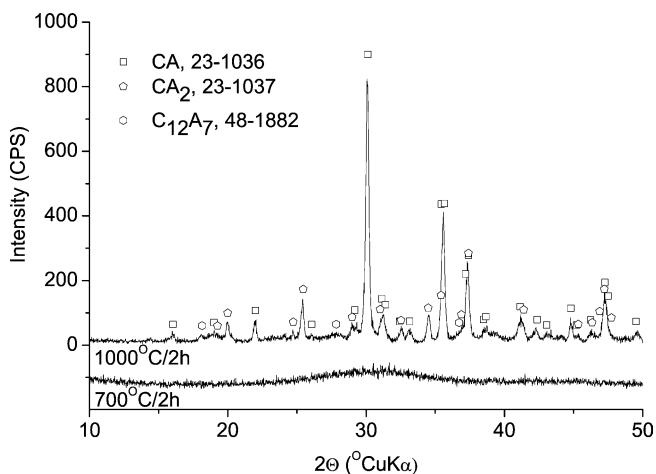


Fig. 4: Powder X-ray diffraction patterns of the sample calcined at 700 °C for 2 h (curve is shifted downwards for visualization purposes), and the calcined sample thermally treated at 1000 °C for 2 h.

In order to determine the crystallization path of the minor phases, the DTA experiment was interrupted at various temperatures and the obtained samples were subjected to XRD. Relative intensities of diffraction peaks normalized within the interval (0,1) and plotted against temperature are shown in Fig. 5. As can be expected, the exotherm between 900 and 1000 °C is associated predominantly with the crystallization of CA, but also CA_2 and C_{12}A_7 . Since all three phases show a constant increase, it can be concluded that simultaneously occurring crystallization processes proceed independently. We believe that the primary reason for formation of minor components in the studied

sample is the inhomogeneity arising from the Al complexing process and salt crystallization. According to Nass and Schmidt ²¹, after hydrolysis of chelated butoxide polycondensation takes place and $[Al(OH)_{3-x}(Eaa)_x]_n$ oligomers are formed. At the same time, the $Ca(NO_3)_2 \times 4H_2O$ crystallizes. In this manner segregated clusters of Ca and Al compounds are formed. Local concentration excess of aluminium and calcium ions results in the formation of aluminium- and calcium-rich phases.

Investigating a similar system, Mohamad ⁶ noted that the minor phases ($C_{12}A_7$ and C_3A) initially increase with time but after reaching the maximum value the amount of these phases subsequently decreased with prolonged firing time. The higher the temperature, the shorter the time to reach the maximum before the amounts of minor phases started to decrease. The behaviour of CA_2 was different, it was observed at all temperatures investigated, but only in relatively small amounts. After initial formation the amount of CA remained almost constant with increasing firing time. In order to obtain an insight into those processes for the investigated gel, calcined samples were placed in platinum crucibles and heated in a furnace isothermally in static air at the temperature of 1500 °C for 2 and 8 h. The fired samples were subsequently subjected to X-ray diffraction analysis. Fig. 6 shows XRD patterns for the thermally treated powders. The intensity of the reflections of CA are enhanced, those of CA_2 are hardly observed and those of $C_{12}A_7$ completely vanish with the annealing at temperature of 1500 °C. Prolonged annealing at the same temperature yielded no change in the relative intensities of those two crystal phases.

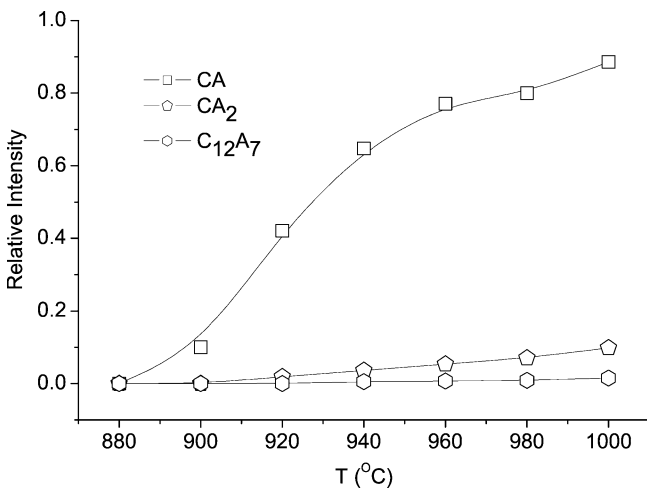


Fig. 5: Relative intensities of XRD peaks (-123 and 220 for CA, -311 for CA_2 and 211 for $C_{12}A_7$) to silicon (111 peak) vs. quenching temperature. Lines are introduced as a guideline for the eye.

The fact that multiple phases crystallize simultaneously presents a serious obstacle to the reliability of kinetic analysis based on DTA measurements. On the other hand, the CA phase predominates, opening the possibility to perform kinetic analysis neglecting the presence of other phases. Therefore, the DTA curves of gels calcined at 700 °C were recorded at heating rates 2, 4, 8, 16, and 32 °C min⁻¹. All the DTA traces exhibit a single endothermic peak at interval between 900 and 1000 °C attributed to crystallization process. The crystallization kinetics is

usually interpreted in terms of the standard nucleation-growth model formulated by Johnson, Mehl and Avrami (JMA) ^{32,33}. Malek ¹⁸ has proposed a testing method to examine the applicability of the JMA model. He introduced the function $z(\alpha) = (d\alpha/dt)T^2$, where α is the volume fraction crystallized, $d\alpha/dt$ the transformation rate, and T is the temperature corresponding to a selected α . Malek has shown that in the case of the JMA model the maximum of the function $z(\alpha)$ should be confined to the interval $0.62 < \alpha < 0.64$. Fig. 7 shows the $z(\alpha)$ values normalized within the interval (0,1) and plotted as a function of α corresponding to different heating rates. It is evident that normalized plots have a maximum within the range of $0.43 < \alpha < 0.61$, which indicates that the non-isothermal crystallization mechanism of the investigated sample cannot be described within the JMA model. Moreover, there are noticeable differences in shape among the curves for different heating rates, which can be attributed to the presence of multiple phases as well as differences in the crystallization mechanism at various heating rates.

The data are further tested using the Kissinger-Akahira-Sunose (KAS) equation ^{19,20}. According to KAS the activation energy for crystallization is related to the heating

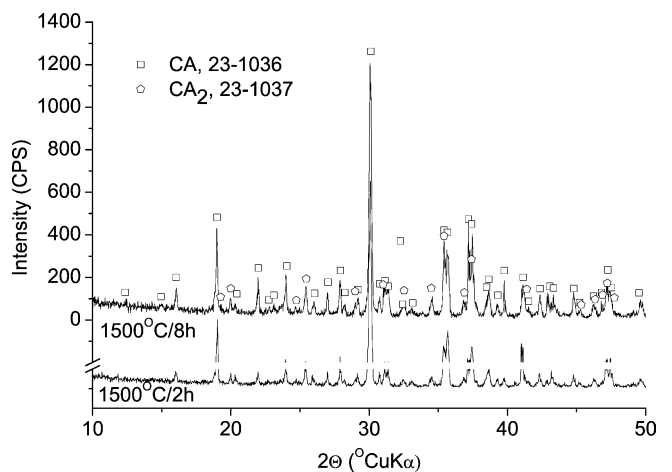


Fig. 6: Powder X-ray diffraction patterns of calcined samples thermally treated at 1500 °C for 2 h (curve is shifted downwards for visualization purposes), and 1500 °C for 8 h.

rate and temperature corresponding to particular degree

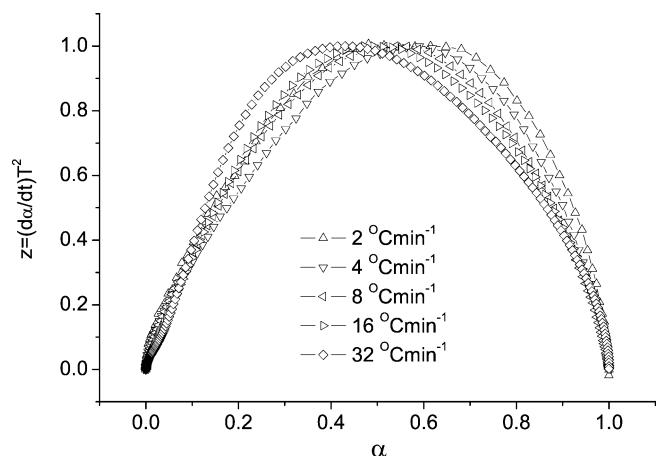


Fig. 7: Plots of function $z(\alpha) = (d\alpha/dt)T^2$ vs. α for the crystallization of an investigated sample at different heating rates.

of conversion through equation: $\ln(\beta/T_\alpha^2) = -(E_\alpha/RT_\alpha) + \text{const}_\alpha$. For each degree of the conversion, α , a corresponding T_α , for various heating rates, β , is used to plot $\ln(\beta/T_\alpha^2)$ against $1/T_\alpha$. The plot should be a straight line the slope of which can be used to calculate the activation energy E_α . When the KAS isoconversional method was applied, a pronounced variation in the slopes of the straight lines, indicating variations of activation energy, with the degree of conversion α is observed. The variation of activation energy with the degree of conversion is shown in Fig. 8.

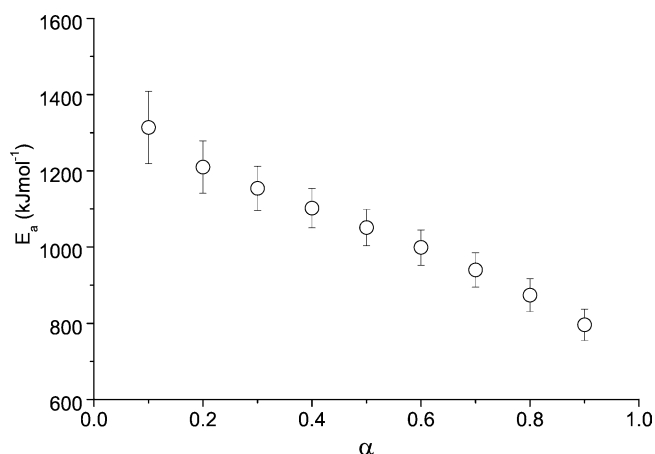


Fig. 8: Variation of apparent activation energy with degree of conversion, α .

From the observed $z(\alpha)$ plots and E_α variations, it is evident that the amorphous-to-crystalline transformation cannot be described by a simple mechanism. Complex reactions involving several processes with different activation energies and mechanisms are involved in the overall crystallization process. Therefore, kinetic analysis in which the activation energy and crystallization mechanism are assumed to be constant is not appropriate to describe the present data and a model cannot be used to extract the true value of activation energy.

IV. Conclusion

The thermal evolution of CA gel prepared using calcium nitrate tetrahydrate and aluminium sec-butoxide as precursors and ethyl acetoacetate as chelating agent was investigated.

The decomposition of the chelate and the evaporation of ethyl acetoacetate take place at temperatures between 100 and 230 °C. An auto-combustion process, associated with sharp exothermic peak and abrupt mass loss, occurs in a narrow temperature range between 230 and 250 °C. The crystallization process starts at temperatures higher than 900 °C. After thermal treatment of the calcined powder at 1000 °C for 2 h, calcium aluminate, CaAl_2O_4 , appears as a major crystalline phase, and calcium dialuminate, CaAl_4O_7 , and dodecacalcium heptaaluminate, $\text{Ca}_{12}\text{Al}_{14}\text{O}_{33}$, as minor phases. The crystallization processes of all three phases proceed simultaneously and independently.

The occurrence of aluminium- and calcium-rich phases in stoichiometric CA gel is assigned to local segregation

owing to a formation of $[\text{Al}(\text{OH})_{3-x}(\text{Eaa})_x]_n$ oligomers and crystallization of $\text{Ca}(\text{NO}_3)_2 \times 4\text{H}_2\text{O}$.

Firing of the sample at 1500 °C for 2 h yielded with the increase of CA quantity, a decrease in CA_2 and complete vanishing of C_{12}A_7 . Prolonged annealing at the same temperature resulted in no further changes.

The crystallization kinetics was studied with the DTA technique. Malek's $z(\alpha)$ function was used to test the applicability of the JMA model and the KAS isoconversional method was used to investigate the variation of the effective activation energy with extent of crystallization. Kinetic analysis revealed that the amorphous-to-crystalline transformation in the studied sample cannot be described on the basis of a simple mechanism. Complex reactions involving several processes with different activation energies and mechanisms are involved in the overall crystallization process.

Acknowledgement

The financial support of the Ministry of Science, Education and Sports of Republic of Croatia within the framework of the project No. 125-1252970-2981 "Ceramic nanocomposites obtained by sol-gel process" is gratefully acknowledged. The authors are much obliged to Prof. J. Macan for the fruitful discussion.

References

- Pati, R.K., Panda, A.B., Pramanik, P.: Preparation of nanocrystalline calcium aluminate powders, *J. Mater. Synth. Proc.*, **10** [4], 157-161, (2002).
- Douy, A., Gervais, M.: Crystallization of amorphous precursors in the calcia-alumina system: A differential scanning calorimetry study, *J. Am. Ceram. Soc.*, **83** [1], 70-76, (2000).
- Goktas, A.A., Weinberg, M.C.: Preparation and Crystallization of Sol-Gel Calcia-Alumina Compositions, *J. Am. Ceram. Soc.*, **74** [5], 1066-1070, (1991).
- Löf, J., Svahn, F., Jarmar, T., Engqvist, H., Pameijer, C.H.: A comparative study of the bioactivity of three dental materials, *Dent. Mater.*, **24** [5], 653-659, (2008).
- Stephan, D., Wilhelm, P.: Synthesis of pure cementitious phases by sol-gel process as precursor, *Z. Anorg. Allg. Chem.*, **630**, 1477-1483, (2004).
- Mohamad, B.M., Sharp, J.H.: Kinetics and Mechanism of Formation of Tricalcium Aluminate, $\text{Ca}_3\text{Al}_2\text{O}_6$, *Thermochim. Acta*, **388**, 105-114, (2002).
- Gülgün, M.A., Popoola, O.O., Kriven, W.M.: Chemical Synthesis and Characterization of Calcium Aluminate Powders, *J. Am. Ceram. Soc.*, **77** [2] 531-39, (1994).
- Sung, Y.-M., Sung, J.-H.: Crystallization behaviour of calcium aluminate glass fibres, *J. Mater. Sci.*, **33**, 4733-4737, (1998).
- Yi, H.C., Guigne, J.Y., Moore, J.J., Schowengerdt, F.D., Robinson, L.A., Manerbino, A.R.: Preparation of calcium aluminate matrix composites by combustion synthesis, *J. Mater. Sci.*, **37**, 4537-4543, (2002).
- Uberoi, M., Risbud, S.H.: Processing of amorphous calcium aluminate powders at <900 °C, *J. Am. Ceram. Soc.*, **73**, 1768-1770, (1990).
- Kerns, L., Weinberg, M.C., Mayers, S., Assink, R.: Al coordination in sol-gel and conventional calcium aluminate glasses, *J. Non-Cryst. Solids*, **232-234**, 86-92, (1998).
- Aitasalo, T., Hölsä, J., Jungner, H., Lastusaari, M., Niittykoski J.: Comparison of sol-gel and solid-state prepared Eu^{2+} doped calcium aluminates, *Mater. Sci.*, **20** [1], 15-20, (2002).

- 13 Haridas, M.M., Goyal, N., Bellare, J.R.: Chemical Synthesis of Optical Grade Ceramic Precursors: A Spectrophotometric Approach for Analysis, *Ceram. Int.*, **24**, 415-420, (1998).
- 14 Bonhomme-Coury, L., Babonneau, F., Livage, J.: Investigation of the sol-gel chemistry of ethylacetoacetate modified aluminum sec-butoxide, *J. Sol-Gel Sci. Tech.*, **3**, 157-168, (1994).
- 15 Tadanaga, K., Iwami, T., Toghe, N., Minami, T.: Precursor structure and hydrolysis-gelation process of $\text{Al}(\text{O-sec-Bu})_3$ modified with ethylacetoacetate, *J. Sol-Gel Sci. Tech.*, **3**, 5-10, (1994).
- 16 Babonneau, F., Coury, L., Livage, J.: Aluminum sec-butoxide modified with ethylacetoacetate: An attractive precursor for the sol-gel synthesis of ceramics, *J. Non-Cryst. Solids*, **121**, 153-157, (1990).
- 17 Kurajica, S., Mali, G., Gazivoda, T., Sipusic J., Mandic, V.: A spectroscopic study of calcium aluminate gels obtained from aluminium sec-butoxide chelated with ethyl acetoacetate in various ratios, *J. Sol-Gel Sci. Tech.*, **50**, 58-68, (2009).
- 18 Malek, J.: The applicability of Johnson-Mehl-Avrami model in the thermal analysis of the crystallization, kinetics of glasses, *Thermochim. Acta*, **267**, 61-73, (1995).
- 19 Kissinger, H.E.: Variation of Peak Temperature with Heating Rate in Differential Thermal Analysis, *J. Res. Nat. Bureau Standards*, **57**, 217-221, (1956).
- 20 Akahira, T., Sunose, T.: Paper No. 246, 1969 Research Report, Trans. Joint Convention of Four Electrical Institutes, Chiba Institute of Technology, **16**, 22-31, (1971).
- 21 Nass, R., Schmidt, H.: Synthesis of an alumina coating from chelated aluminium alkoxides, *J. Non-Cryst. Solids*, **121**, 329-333, (1990).
- 22 Silverstein, R.M., Webster, F.X.: Spectrometric Identification of Organic Compounds, 6th edition, J. Wiley & Sons Inc., New York, (1998).
- 23 González Peña, V., Márquez-Alvarez, C., Diaz, I., Grande, M., Blasco, T., Pérez-Pariente, J.: Sol-gel synthesis of mesostructured aluminas from chemically modified aluminum sec-butoxide using non-ionic surfactant templating, *Microporous Mesoporous Mater.*, **80**, 173-182, (2005).
- 24 Jackson, P., Carter, D., Dent, G., Cook, B.W., Chalmers, J.M., Dunkin, I.R.: Selective thermolysis of the enol forms of acetoacetates during gas chromatography, revealed by combined matrix-isolation Fourier transform infrared and mass spectrometry, *J. Chromatogr. A*, **685**, 287-293, (1994).
- 25 Jing, C., Zhao, X., Zhang, Y.: Sol-gel fabrication of compact, crack-free alumina film, *Mater. Res. Bull.*, **42**, 600-608, (2007).
- 26 Durán, P., Tartaj, J., Rubio, F., Moure, C., Peña, O.: Synthesis and sintering behaviour of spinel-type $\text{Co}_x\text{NiMn}_{2-x}\text{O}_4$ ($0.2 \leq x \leq 1.2$) prepared by the ethylene glycol-metal nitrate polymerized complex process, *Ceram. Int.*, **31**, 599-610, (2005).
- 27 Hosseini Vajargah, S., Madaah Hosseini, H.R., Nemati, Z.A.: Preparation and characterization of yttrium iron garnet (YIG) nanocrystalline powders by auto-combustion of nitrate-citrate gel, *J. Alloys Comp.*, **430**, 339-343, (1997).
- 28 Yang, T., Wang, H., Lei, M.K.: Phase transition of Er^{3+} -doped Al_2O_3 powders prepared by the non-aqueous sol-gel method, *Mater. Chem. Phys.*, **95**, 211-217, (2006).
- 29 Zawrah, M.F., Khalil, N.N.: Synthesis and characterization of calcium aluminate nanoceramics for new applications, *Ceram. Int.*, **33**, 1419-1425, (2007).
- 30 Singh, K., Ali, M.M., Mandal, U.K.: Formation Kinetics of Calcium Aluminates, *J. Am. Ceram. Soc.*, **73** [4], 872-876, (1990).
- 31 Scian, A.N., Porto-López, J.M., Pereira, E.: High alumina cements. Study of $\text{CaO} \cdot \text{Al}_2\text{O}_3$ formation. I. Stoichiometric mechanism, *Cem. Concr. Res.*, **17**, 198-204, (1987).
- 32 Avrami, M.: Granulation, phase change and microstructure: Kinetics of phase change (III), *J. Chem. Phys.*, **9**, 177-184, (1941).
- 33 Johnson, W.A., Mehl, R.F.: Reaction kinetics in processes of nucleation and growth, *Trans. Am. Inst. Miner. (Metall.) Eng.*, **135**, 416-458, (1939).

